Earth and Planetary Science Letters 430 (2015) 377–386

Contents lists available at ScienceDirect

Earth and Planetary Science Letters

www.elsevier.com/locate/epsl

Bahamian speleothem reveals temperature decrease associated with Heinrich stadials

Monica M. Arienzo [a,b,*], Peter K. Swart [a], Ali Pourmand [a], Kenny Broad [c], Amy C. Clement [d], Lisa N. Murphy [d], Hubert B. Vonhof [e], Brian Kakuk [f]

[a] Department of Marine Geosciences, Rosenstiel School of Marine and Atmospheric Science, University of Miami, 4600 Rickenbacker Causeway, Miami, FL, USA
[b] Division of Hydrologic Sciences, Desert Research Institute, Reno, NV, USA
[c] Department of Marine Ecosystems and Society, Rosenstiel School of Marine and Atmospheric Science, University of Miami, 4600 Rickenbacker Causeway, Miami, FL, USA
[d] Department of Atmospheric Sciences, Rosenstiel School of Marine and Atmospheric Science, University of Miami, 4600 Rickenbacker Causeway, Miami, FL, USA
[e] Faculty of Earth and Life Sciences, Vrije Universiteit Amsterdam, De Boelelaan 1085, 1081 HV Amsterdam, The Netherlands
[f] Bahamas Underground, Marsh Harbor, Bahamas

ARTICLE INFO

Article history:
Received 21 October 2014
Received in revised form 7 August 2015
Accepted 26 August 2015
Available online xxxx
Editor: G.M. Henderson

Keywords:
speleothem
Heinrich event
stable isotope
fluid inclusion
Bahamas

ABSTRACT

Temperature reconstructions across Heinrich stadials 1–3 are presented from an absolute-dated speleothem from Abaco Island in the Bahamas to understand the nature of climate change across these intervals in the subtropical Atlantic. The stalagmite carbonate record, dated by the U–Th geochronometry technique, includes higher $\delta^{18}O$ and $\delta^{13}C$ values within Heinrich stadials 1, 2, and 3 followed by rapid declines at the end of the stadials. To aid in the interpretation of these results, the $\delta^{18}O$ of fluid inclusions associated with the Heinrich stadials were also analyzed. These measurements, which allowed for the relative influence of temperature and $\delta^{18}O$ of precipitation to be distinguished, demonstrate minimal changes in the $\delta^{18}O$ of fluid inclusions, suggesting that changes in the $\delta^{18}O$ values of the speleothem carbonate associated with Heinrich stadials 1–3 are principally driven by an average ~4 °C temperature decrease, rather than a change in the $\delta^{18}O$ of the rainfall (hence rainfall amount). These findings support previous work in the North Atlantic and are consistent with the climate response to a weakening of the Atlantic meridional overturning circulation.

1. Introduction

Ice core and deep sea sediment records of the last 65 000 years show 18 periods of millennial scale climate events known as the Dansgaard/Oeschger (D/O) cycles and 6 Heinrich stadials (Dansgaard et al., 1984). Dansgaard/Oeschger events in Greenland are millennial scale alternations between warm (interstadial) and cold (stadial) periods (Bond et al., 1997). Heinrich events are characterized in the North Atlantic by cold periods, and are recognized in the sedimentary record as eroded terrigenous materials (Ice Rafted Debris, IRD) deposited in the North Atlantic by icebergs upon melting (Bond et al., 1997; Heinrich, 1988). Heinrich stadials are associated with a slowdown of the Atlantic meridional overturning circulation (AMOC) and an inter-hemispheric climate response (Wolff et al., 2010; McManus et al., 2004). Observations and models (Zhang and Delworth, 2005) support reduction in sea surface temperatures (SSTs) associated with Heinrich stadials, thought to be caused by reduced northward heat transport, driven by the slowdown of the AMOC (Clement and Peterson, 2008) or the increase in sea/land ice (Chiang and Bitz, 2005). Reduced Northern Hemisphere SSTs led to the southward shift in the intertropical convergence zone (ITCZ) and drier conditions in the tropical Northern Hemisphere (Chiang and Bitz, 2005; Stager et al., 2011). Recent studies have also demonstrated the impact of varying height of the Laurentide ice sheet as a climate forcing during Heinrich stadial events (Roberts et al., 2014). During interstadial periods (i.e. D/O interstadial events), the inverse occurs with a poleward shift of the Northern Hemisphere summer ITCZ and the jet streams (Asmerom et al., 2010). However, the exact mechanisms driving these events are still not well understood (Clement and Peterson, 2008).

Various types of paleoclimate data support the global response to North Atlantic Heinrich stadials, as well as the abrupt nature of the events. Paleoclimate records suggest that the global signature of Heinrich stadials includes: a drier Europe (Genty et al., 2003), weaker Asian monsoon (Wang et al., 2001), wetter

* Corresponding author.
E-mail address: marienzo@dri.edu (M.M. Arienzo).

http://dx.doi.org/10.1016/j.epsl.2015.08.035
0012-821X/

southwestern North America (Asmerom et al., 2010; McGee et al., 2012), drier northern South America (Peterson et al., 2000), wetter southern South America (Kanner et al., 2012), an overall drier tropical Asia and Africa (Stager et al., 2011), and a gradually warming Antarctica (Wolff et al., 2010) (for a review of paleoclimate data across Heinrich stadials see Clement and Peterson, 2008). While a comprehensive picture of climate across North Atlantic Heinrich stadials is emerging from records in both hemispheres, very few studies have been conducted in the subtropical western Atlantic (Grimm et al., 2006; Lachniet et al., 2013; Sachs and Lehman, 1999), which may be an important area for detecting the global propagation of these events and constraining climate models. In this study, geochemical data obtained from a speleothem spanning Heinrich stadials 1–3 are presented from a cave in Abaco Island, Bahamas. Each Heinrich stadial event exhibited unique characteristics, supporting other studies showing Heinrich stadial 1 to be the strongest event (Stager et al., 2011), with almost complete shutdown in AMOC (McManus et al., 2004).

1.1. Speleothems as paleoclimate archives

Speleothems have proven to be valuable archives for paleoclimate reconstructions, particularly for the study of climate variability on millennial timescales (Asmerom et al., 2010; Wang et al., 2001). Stable isotope ratios of oxygen and carbon ($\delta^{18}O$ and $\delta^{13}C$) of the carbonate are the most common geochemical proxies analyzed within speleothems. There are several climate factors that can lead to changes in the $\delta^{18}O$ values of the carbonate record. In the case of tropical speleothems, the $\delta^{18}O$ of the carbonate is typically interpreted to be driven primarily by the $\delta^{18}O$ of the rainfall and/or the temperature of the cave (Kanner et al., 2012; van Breukelen et al., 2008), and studies have shown that cave drip water has $\delta^{18}O$ values similar to local precipitation (Tremaine et al., 2011; van Breukelen et al., 2008). In the Bahamas and throughout the Caribbean and south Florida, there is an inverse relationship between the amount of rainfall and the $\delta^{18}O$ of the rainwater (Baldini et al., 2007; van Breukelen et al., 2008), and therefore the amount of rainfall (the amount effect) is considered to exert the main control on the $\delta^{18}O$ composition of the rainfall precipitation (Dansgaard, 1964). However, distinguishing the competing influences of temperature and $\delta^{18}O$ of the rainwater is inherently complex when interpreting the carbonate $\delta^{18}O$ results. One approach to address the confounding influences of temperature and water $\delta^{18}O$ is through the $\delta^{18}O$ analysis of fluid inclusions. These inclusions are microscopic water filled cavities located within the speleothem calcite mineral structure which contain drip water trapped at the time the stalagmite formed. As suggested above, the drip water is thought to directly represent precipitation, and therefore the isotopic analysis of the trapped water provides a direct measure of the temporal changes in the $\delta^{18}O$ of rainfall (hence rainfall amount). Determining the $\delta^{18}O$ value of both the trapped fluid and that of the accompanying mineral allows the temperature at the time of speleothem formation to be calculated (van Breukelen et al., 2008).

In contrast, the $\delta^{13}C$ of the carbonate is a function of the type and amount of vegetation above the cave, root respiration, organic material decomposition, the amount of water/rock interactions and prior calcite precipitation (Fairchild et al., 2006). Variation in the biogenic CO_2 component of the carbon is in turn influenced by precipitation amount and temperature (Genty et al., 2003). Generally the partial pressure of CO_2 (pCO_2) is expected to show an inverse correlation with $\delta^{13}C$ values in the soil horizon. Changes in the amount of rainfall or temperature could also alter the ratio of C_3 and C_4 plants, causing further isotopic changes, particularly over longer timescales (Fairchild et al., 2006). Cave ventilation may also exert control over the $\delta^{13}C$ of the CO_2 in the cave and therefore ultimately the $\delta^{13}C$ in the cave fluids (Tremaine et al., 2011). Through the combination of both $\delta^{18}O$ and $\delta^{13}C$ of the carbonate as well as $\delta^{18}O$ of the fluid inclusions, variations in the temperature and amount of rainfall can be estimated over the sample time period.

1.2. Previous work on Bahamian speleothems

Several studies have been conducted on the formation, growth, age, and geochemistry of Bahamian speleothems, with most of the work carried out on samples from caves currently submerged in seawater (Richards et al., 1994 and references therein). These speleothems formed during previous sea level low-stands and stopped forming when rising sea level flooded the caves, making the speleothems potential archives of paleo-sea level. However, it has also been shown in some instances that the speleothems ceased forming prior to seawater flooding, presumably as a result of drier conditions (Richards et al., 1994). Richards et al. (1994) also found no geochemical evidence of alteration in samples from submerged caves. Stalagmites from the Bahamas have been additionally utilized as recorders of past atmospheric $\Delta^{14}C$ concentration for radiocarbon calibrations (Hoffmann et al., 2010; Beck et al., 2001).

The aim of this work is to determine the paleoclimatic changes associated with Heinrich stadials over the last ~32 000 years by applying multiple geochemical tools. This study represents the first high resolution paleoclimate reconstruction utilizing a Bahamian speleothem and the first multi-collector ICP-MS dated speleothem from this region. Additionally, the combination of both stable isotope analyses of the carbonate and fluid inclusions is unique and the resolution of the fluid inclusion analyses for a stalagmite record from this time period is unprecedented. Finally, considering that relatively few studies have been conducted in the subtropical western Atlantic (Escobar et al., 2012; Grimm et al., 2006; Hagen and Keigwin, 2002; Hodell et al., 2012; Keigwin and Jones, 1994; Sachs and Lehman, 1999), and even fewer studies are from terrestrial records, this study offers the opportunity to better understand abrupt climate change at this location during the Pleistocene and its relationship to the climate of the North Atlantic.

2. Sample locality and methods

2.1. Regional setting

The modern climate of the Bahamas is primarily controlled by the easterly trade winds and winds from the west are limited to frontal passages (Baldini et al., 2007). The annual variation in air temperature ranges from 22 to 28 °C (Baldini et al., 2007). There are distinct wet and dry seasons with the wetter period between April to December driven by the Bermuda high.

The stalagmite (sample AB-DC-09) was collected from a currently submerged cave located in the middle of southern Abaco Island, Bahamas (N26°14, W77°10) in July of 2007 from a depth of 16.5 m below current sea level (Fig. 1). The cave is accessed through a collapsed sinkhole and consists of three laterally extensive levels at ~22, 33.5 and 45 m below sea level. The overlying bedrock of the cave is composed of Pleistocene limestone aeolianites and marine limestones (Walker et al., 2008). After collection, the speleothem was sectioned along the main growth axis (Fig. 2a) and sampled in the central region for U–Th geochronometry, stable C and O isotopes ($\delta^{13}C_c$ and $\delta^{18}O_c$), and $\delta^{18}O_w$ of fluid inclusions. Sample AB-DC-09 has a total length of 23 cm and is comprised of dense milky white calcite with no evidence of post-depositional diagenesis (Fig. 2a).

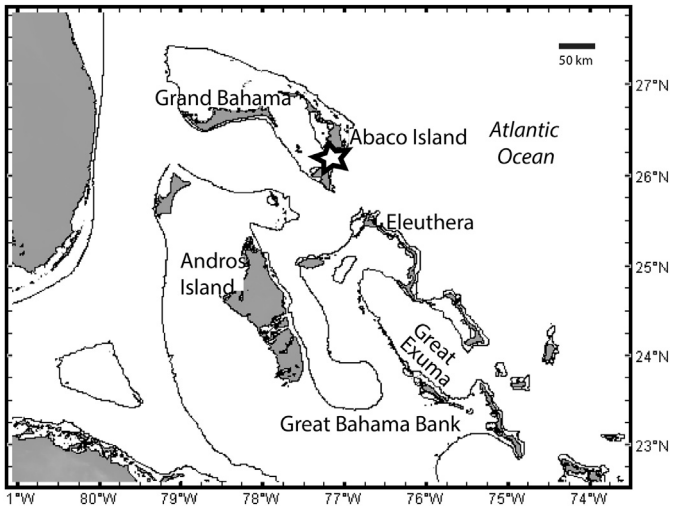

Fig. 1. Sample AB-DC-09 was collected from Abaco Island in the Bahamas (N26°14, W77°10). Cave location is indicated by the star. Contours show 120 m bathymetry.

2.2. Geochemical methods

2.2.1. U–Th geochronometry

Twenty-three U–Th dates (Table 1) were measured at the Neptune Isotope Laboratory of the University of Miami – RSMAS utilizing a ThermoFisher-Neptune Plus multi-collector ICP-MS. Details of the U–Th geochronometry technique and propagation of random and systematic uncertainties are discussed elsewhere (Pourmand et al., 2014). Briefly, 100–200 mg of the sample was hand-drilled. Samples were then completely digested in 5 mL of 6 mol L^{-1} HNO_3 followed by the addition of ~0.5 g of a previously calibrated ^{229}Th–^{233}U–^{236}U spike mixture. The concentrations of U and Th in the spike solution were determined by isotope dilution mass spectrometry against a mixture of U and Th mono-elemental standard solutions and gravimetrically prepared U standard from ~1 g of U metal (full details on spike calibration are provided in Pourmand et al. (2014)). To separate U and Th from matrix elements (mainly Ca, Sr and Mg), the sample and spike mixture were loaded on to pre-packed 2-mL cartridges of U/TEVA resin (particle size 50–100 µm) from Eichrom Inc. After removal of the matrix elements, Th and U were quantitatively separated from each other in 10 mL of 3 and 0.1 mol L^{-1} HCl, respectively.

Higher abundance U (^{233}U, ^{235}U, ^{236}U and ^{238}U) and Th (^{229}Th, ^{232}Th) isotopes were measured in Faraday collectors while ^{234}U and ^{230}Th isotopes were measured in the secondary electron multiplier (SEM) after the ion beams passed through a Retardation Potential Quadrupole (RPQ) filter to reduce the abundance sensitivity effect. Each U and Th measurement was bracketed by two measurements of inlet system memory from previous runs and measurements of CRM-112A and IRMM-035 standard solutions spiked with IRMM-3636a ^{233}U–^{236}U double spike. Data acquisition for U and Th isotopes and the half-masses were exported to Excel

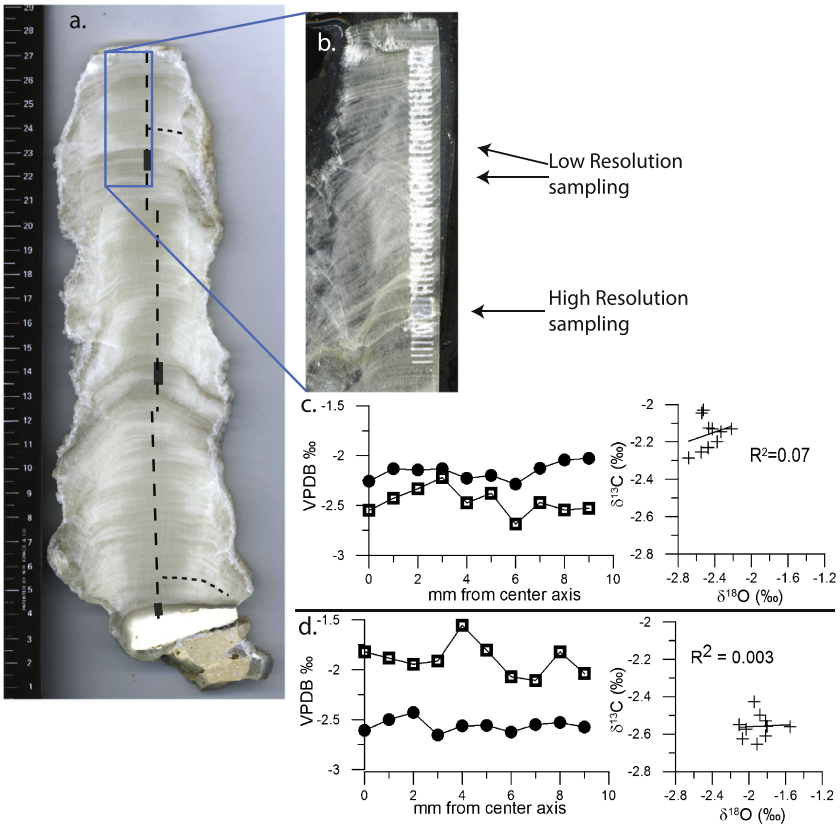

Fig. 2. a) Photo of sample AB-DC-09 showing the sampling locations: dashed line represents low resolution analysis, black bars represent high resolution analysis, and horizontal dotted lines represent the location of Hendy tests. b) Photo of thin section after sampling for geochemical analysis of the upper most section of the speleothem. This demonstrates areas of both high and low resolution $\delta^{18}O_c$ and $\delta^{13}C_c$ analyses. Along the center axis, millimeter scale laminations of the speleothem calcite are found. Microscopic analysis displays no evidence of post depositional alteration or evidence of a hiatus in the center. However, along the outer most portion of the stalagmite, blocky calcite is observed with minimal layering, suggesting this area may be affected by post-depositional diagenesis. c) Hendy test results from 3 cm from the top showing variation in carbon and oxygen isotopes (black circles and open squares respectively) from the center of the growth axis outward along a growth band, showing little variation in both carbon and oxygen isotopes. Also shown is low correlation between carbon and oxygen isotopes. d) Hendy test results from 23 cm from the top showing carbon and oxygen isotopes (black circles and open squares respectively) from the center of the growth axis outward, with little variation and low correlation across a growth band.

spreadsheet templates and processed using an open-source algorithm in Mathematica as presented in Pourmand et al. (2014) for calculating the U and Th concentrations, age and uncertainties (reported here as 95% confidence interval). A significant advantage of this technique is consideration for U and Th isotope covariance and propagation of uncertainties on decay constants and other sources of random and systematic uncertainties on corrected ages, which are especially crucial for comparison with age models that are not based on U–Th geochronometry. The half-life values used are those presented in Edwards et al. (2003) and Fietzke et al. (2005). The concentration of U and Th in procedural blanks, which were processed every five samples, were below 1 and 10 pg, respectively, and therefore no blank corrections were necessary. All ages are reported in years before present (yr BP).

2.2.2. Isotopic sampling on the carbonate

Sampling of the speleothem carbonate for $\delta^{13}C_c$ and $\delta^{18}O_c$ (calcite) was carried out using a New-Wave computerized micromill at both high and low resolution. Low resolution sampling consisted of one individual sample every 1000 µm (Fig. 2a and b). The low resolution analysis revealed three areas of rapid and significant isotopic shifts. These areas were subsequently analyzed at a higher resolution (20 µm sampling interval) for a total of ~550 high resolution samples (Fig. 2b). Isotopic measurements were made using a Kiel III interfaced with a Thermo-Finnigan Delta Plus Mass Spectrometer at the University of Miami. All data have been corrected for isobaric inferences at mass 45 and 46 and $\delta^{13}C_c$ and $\delta^{18}O_c$ values are reported relative to Vienna Pee Dee Belemnite (VPDB). The error for these analyses is < 0.1‰ as determined by repeated measurement of an internal standard.

2.2.3. Fluid inclusions

Thirty-one oxygen and hydrogen isotopic analyses of the fluids trapped within inclusions ($\delta^{18}O_w$ and $\delta^{2}H_w$) were carried out at the University of Miami using a cavity ring-down spectroscopy instrument (L2130-i Picarro) as outlined in Arienzo et al. (2013). This system allowed for the determination of $\delta^{18}O$ of the water ($\delta^{18}O_w$) and $\delta^{2}H_w$ of the fluid inclusions from approximately 0.2 g samples, which on average yielded 0.4 µL of water from AB-DC-09 speleothem. Sampling for fluid inclusion analysis was conducted along the center of the growth axis, utilizing a band saw to extract 0.6–1.0 g cubes of calcite which were subsequently divided into ~0.2 g cubes for replicate analysis. The isotopic compositions of the fluid inclusions are reported relative to the Vienna Standard Mean Ocean Water (VSMOW). Each sample was analyzed 1–3 times with an average error of 0.5‰ for $\delta^{18}O_w$ and 2.0‰ for $\delta^{2}H_w$ values (Arienzo et al., 2013). As a result of the larger sample size, average sampling was conducted every 0.75 cm. The $\delta^{18}O_c$ of the calcite hosting the inclusion was measured on the crushed residue at the University of Miami using a Thermo-Finnigan Delta Plus mass spectrometer (see above).

3. Results

3.1. Age model

3.1.1. Unsupported ^{230}Th

An important variable in U–Th geochronometry is the contribution of excess (unsupported) ^{230}Th to the U series equilibrium clock (Edwards et al., 2003). Isochron techniques and direct measurements from modern cave deposits provide estimates of the initial ^{230}Th. Previous studies of Bahamian speleothems forming over the last glacial maximum (LGM) utilizing isochrons suggested relatively high initial ^{230}Th/^{232}Th activity ratios, ranging from 7.8 ± 4.0 (Hoffmann et al., 2010) to 18.7 ± 2.9 (Beck et al., 2001). These samples were collected from Grand Bahama Island, located to the north of Abaco Island and were forming over the LGM. Rather than conducting isochrons, which require identifying cogenetic samples of homogeneous parent and daughter composition within the same depositional horizon (Edwards et al., 2003), we have analyzed modern cave calcites from an actively forming cave in Eleuthera, Bahamas in order to determine a representative ^{230}Th detrital activity ratio. The results measured in the depositional slides yielded an average initial ^{230}Th/^{232}Th activity ratio of 2.2 ± 0.6 (Supplementary material). These findings from speleothems suggest that, for the Bahamas, there is a wide range of measured initial ^{230}Th/^{232}Th activity ratios from 2.2 to 18.7. The published data with higher initial ^{230}Th/^{232}Th activity ratios were from samples that were forming over the LGM, suggesting the cave had a higher Th input during this period than the modern samples from Eleuthera. Other studies have characterized the U and Th concentrations in carbonates and waters of the Bahamas, and these studies demonstrate wide variability in concentrations and several potential sources of detrital Th, including aeolian inputs (e.g., Robinson et al., 2004).

Considering that stalagmites from Abaco Island have yet to be studied, comparative data for this island does not exist. Therefore, from the results outlined above, the activity ratio of 3.7 ± 0.6 for initial ^{230}Th/^{232}Th is considered a reasonable estimate as this value falls in the range of values for the Bahamas, and additionally results in good agreement with previously published records. Nevertheless, we further assess the contribution of the initial, unsupported ^{230}Th by a sensitivity test whereby the ages were propagated at various initial (^{230}Th/^{232}Th) ratios (Supplementary Table 2). This sensitivity study demonstrates that the initial Th value does not significantly change the timing of Heinrich stadials 1 or 2, however, a lower activity ratio (e.g., 0.6) resulted in the timing of Heinrich stadial 3 to be an unreasonable age with respect to published ages for the event. Varying the initial ^{230}Th/^{232}Th activity ratio impacts the age calculated on the oldest U–Th ages, and these ages do consist of the largest errors. Given the good agreement with other published records, the activity ratio of 3.7 ± 0.6 for initial ^{230}Th/^{232}Th is considered a reasonable estimate.

It must be noted that we make the assumption that the initial Th activity ratio did not change throughout the deposition of the stalagmite. When propagating the U–Th ages using an activity ratio of 3.7 ± 0.6 for initial ^{230}Th/^{232}Th, three ages showed reversals (Table 1). Two of the ages located ~5 cm from the top were younger than the previous ages, resulting in a reversal (Table 1). This reversal may be driven by a reduction in the initial ^{230}Th/^{232}Th activity ratio component during this time period and therefore we do not include these two dates in the age model. One U–Th age 11 cm from the top was older and resulted in an age reversal, possibly suggesting an increase in the initial ^{230}Th/^{232}Th activity ratio component at this time. Considering the good agreement between surrounding ages, we discount this age as well and do not include it in the final age model.

3.1.2. Age model

Utilizing twenty U–Th ages the final age model was calculated using the Constructing Proxy-Records from Age models (COPRA) program from Breitenbach et al. (2012) (Fig. 3). The age model was calculated in MATLAB® using the Piecewise Cubic Hermite Interpolating Polynomial (PCHIP) and 2000 Monte Carlo simulations to assign a precise timescale (Fig. 3). When plotting the age model with other paleoproxies from the region, we find good agreement in the timing of isotopic shifts between records (discussed in detail in Section 4.3), which further validates the decision to utilize a value of 3.7 ± 0.6 for initial ^{230}Th/^{232}Th activity ratio.

The age model results indicate that the stalagmite grew between 13.8 to 32 kyr before present (Figs. 3 and 4). There is no evidence for any growth hiatuses throughout the sample from ei-

Table 1
Stalagmite AB-DC-09 ^{230}Th dating results for samples dated in the Neptune Isotope Laboratory at the University of Miami (see Pourmand et al., 2014 for detailed methodology), ages have been corrected for a ^{230}Th/^{232}Th activity ratio of 3.7 ± 0.6 to account for detrital ^{230}Th. All uncertainties are calculated as 95% confidence interval (95% CI). Ratios in parentheses are activities.

Distance from top (μm)	^{238}U (ppb)	(95% CI) ±	(^{230}Th/^{238}U)	(95% CI) ±	(^{230}Th/^{232}Th)	(95% CI) ±	Uncorr. age (yr)	(95% CI) ±	(^{234}U/^{238}U) initial (corrected)	(95% CI) ±	Corr. age (yr)	(95% CI) ±
17 000	201.838	0.124	0.1332	0.0007	57.6	0.94	15 394	77	1.0131	0.00259	14 468	166
35 000	179.526	0.097	0.1360	0.0006	54.5	1.56	15 882	71	1.0047	0.00267	14 872	178
42 500	209.472	0.103	0.1355	0.0009	66.8	2.30	15 717	110	1.0112	0.00249	14 902	174
60 000	150.938	0.086	0.1552	0.0010	47.9	1.12	18 572	123	0.9921	0.00278	17 244	246
72 500	188.150	0.113	0.1545	0.0014	102.5	1.90	18 054	176	1.0145	0.00251	17 453	198
89 000	204.483	0.108	0.1607	0.0009	43.5	0.27	18 956	109	1.0087	0.00265	17 465	260
95 000	203.633	0.110	0.1569	0.0007	81.8	2.81	18 527	78	1.0053	0.00250	17 753	146
103 000	191.743	0.103	0.1615	0.0009	95.4	4.01	19 043	111	1.0093	0.00248	18 363	156
115 000	245.881	0.129	0.1683	0.0008	144.4	8.89	19 852	96	1.0129	0.00256	19 385	126
124 000	214.688	0.106	0.1732	0.0008	80.7	0.52	20 586	96	1.0085	0.00274	19 722	169
125 000	212.781	0.109	0.1739	0.0009	86.9	3.56	20 597	105	1.0117	0.00255	19 795	168
133 000	180.454	0.083	0.1781	0.0010	77.4	0.96	21 486	120	0.9972	0.00245	20 551	191
137 000	183.408	0.109	0.1876	0.0022	128.6	1.69	22 309	284	1.0159	0.00253	21 727	299
145 000	164.362	0.082	0.1923	0.0010	48.3	0.36	23 646	124	0.9875	0.00258	22 007	294
149 000	179.101	0.104	0.2067	0.0009	47.0	0.85	25 148	100	1.0051	0.00249	23 366	299
156 000	192.366	0.113	0.2210	0.0011	110.9	0.83	26 649	126	1.0215	0.00258	25 859	177
178 000	202.090	0.127	0.2235	0.0011	139.6	0.93	27 030	127	1.0201	0.00252	26 394	162
199 000	204.470	0.150	0.2427	0.0010	38.2	0.17	29 794	122	1.0170	0.00271	27 239	433
210 000	229.838	0.113	0.2435	0.0010	44.5	0.86	30 055	124	1.0125	0.00271	27 849	378
222 000	202.531	0.126	0.2879	0.0013	19.0	0.11	36 204	172	1.0209	0.00261	30 025	1036
Not used in age model:												
50 000	128.045	0.084	0.1324	0.0009	53.9	0.92	15 640	112	0.9918	0.00248	14 633	194
55 000	129.585	0.074	0.1281	0.0006	69.1	2.56	15 145	62	0.9888	0.00251	14 384	138
110 000	211.462	0.127	0.1779	0.0009	79.5	0.55	20 926	110	1.0206	0.00263	20 038	177

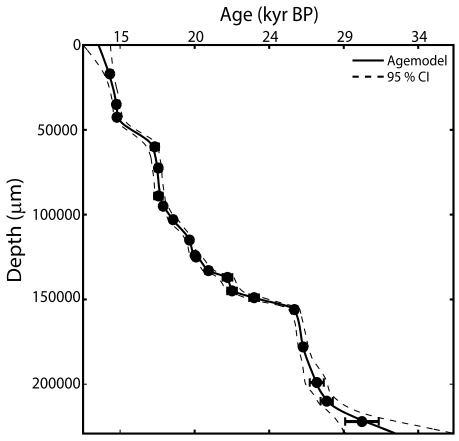

Fig. 3. Age model (black line) based on twenty U–Th ages. The U–Th ages (black dots) are reported with 95% confidence interval which includes random and systematic sources of uncertainty, and the uncertainties on decay constants (see Pourmand et al., 2014 for details). The age model was developed utilizing the COPRA program from Breitenbach et al. (2012). 2000 Monte Carlo simulations were conducted, with the black line representing the mean value and the dotted line representing the 95% confidence interval (Breitenbach et al., 2012).

ther the age measurements or petrographic thin section analysis, however, there is evidence for periods of decreased growth rates from the U–Th geochronometry. The lowest growth rate occurred from 22 to 26 kyr BP (~14.5 to 15.5 cm from top) and two additional periods of decreased growth rate from 14.9 to 17.3 kyr BP (~4.2 to 6 cm from the top) and 27.8 to 30 kyr BP (~21 to 23 cm from the top). There is evidence of three small layers of darker laminations at ~5, 14.5 and 22 cm from the top (Fig. 2a and b) which correlate with the three short periods of reduced calcite precipitation. These layers may represent brief reductions in growth or hiatuses, however do not significantly impact the interpretation of the results (Supplementary Figs. 3 and 4).

3.2. Tests for kinetic fractionation

Several studies have shown that the δ^{18}O and δ^{13}C can be affected by kinetically driven fractionations during the deposition of the carbonate which can overwhelm environmental and climate signals (Hendy, 1971; Lachniet, 2009). An approach often used to examine the role of kinetic effects is known as the "Hendy test" (Hendy, 1971) in which the lateral variation in a chemical parameter within the speleothem is measured. Assuming that sampling can be carried out along a growth band, the following criteria must be met for the Hendy test: i) an absence of lateral increases in $\delta^{18}O_c$ and $\delta^{13}C_c$ values, and ii) a low correlation between $\delta^{18}O_c$ and $\delta^{13}C_c$ values. If these conditions are fulfilled, then it is assumed that minimal kinetic fractionation has taken place. However, studies have demonstrated that this test may not be sufficient to rule out kinetic fractionation (Mühlinghaus et al., 2009). Other authors have suggested a more robust method is to conduct replication tests, in which multiple stalagmites from the same cave are measured and if the $\delta^{13}C_c$ and $\delta^{18}O_c$ trends are replicated, this supports a lack of kinetic fractionation (Dorale and Liu, 2009). For this study, we have conducted the Hendy test and present two locations across which lateral variation of $\delta^{18}O_c$ and $\delta^{13}C_c$ values were measured. Sampling for kinetic fractionation was conducted at one millimeter increments from the center of the growth axis progressing outward along a growth band. As shown in Fig. 2c and d, tests for kinetic fractionation demonstrate low correlation and no significant increase for both $\delta^{13}C_c$ and $\delta^{18}O_c$ across a lamina. This demonstrates that significant fractionation for $\delta^{13}C_c$ and $\delta^{18}O_c$ has not occurred for this speleothem, additionally supported by visual and petrographic observation of the sampled calcite, which is free of evidence of dissolution. In addition, in a cave from Eleuthera in the Bahamas where there is currently active stalagmite formation, the measured δ^{18}O of the calcite, the temperature of the cave, and drip water δ^{18}O all support the idea that the calcite is precipitated in equilibrium (Supplementary text).

For fluid inclusions, isotopic fractionation after deposition can occur through fractionation between the water and the surround-

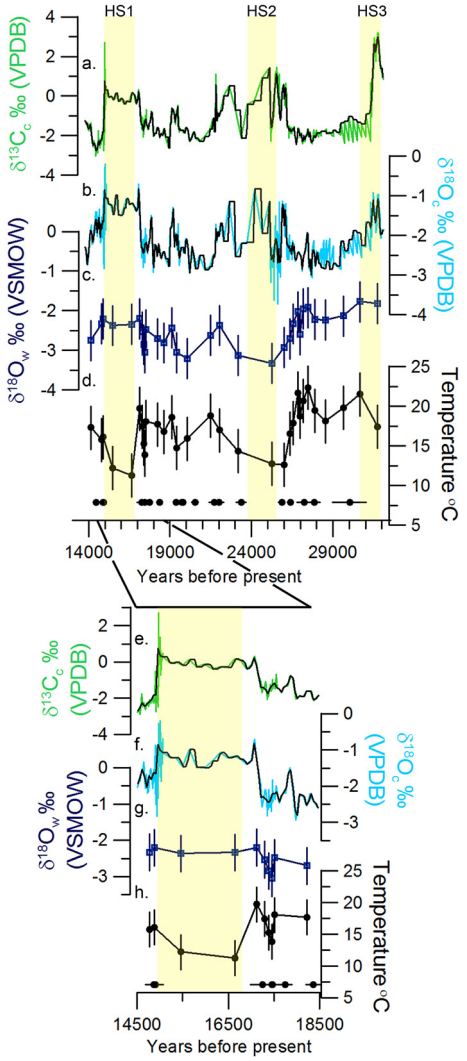

Fig. 4. a) and b) Carbon isotope values of the carbonate (green) time series from AB-DC-09 plotted with $\delta^{18}O_c$ (blue) from the same sample, with 50 yr interpolation in black. c) Dark blue squares are fluid inclusion $\delta^{18}O_w$ water results. d) Average temperature from fluid inclusion results is shown in the solid black line, calculated using the equation from Tremaine et al. (2011). e–h) Same as a–d) from 18 500 to 14 500 yr BP. Yellow bars are Heinrich stadials (HS) 1, 2 and 3. (For interpretation of the references to color in this figure legend, the reader is referred to the web version of this article.)

ing calcite, thereby altering the isotopic composition of the trapped water. However, such fractionation in the humid subtropics should be minimal (van Breukelen et al., 2008). The fluid inclusions are representative of paleoprecipitation, therefore results should fall on the global meteoric water line (GMWL), which defines the linear $\delta^{18}O_w$ versus δ^2H_w relationship for all meteoric waters (Craig, 1961). Fluid inclusion results plot near the GMWL, suggesting that the $\delta^{18}O_w$ and δ^2H_w values have not been affected by fractionation and the data are therefore representative of the original meteoric water composition (Fig. 5).

Precipitation rate can influence kinetic fractionation if the rate of precipitation is faster than the rate of HCO_3^-(aq) re-equilibration, which may impact the fluid inclusion results. However, given the lack of evidence for kinetic fractionation from the carbonate isotopes, it is not thought that kinetic fractionation is a significant driver of the chemistry. In addition, Baldini et al. (2007) demonstrated that the $\delta^{18}O_w$ of rainwater from San Salvador, Bahamas varied between −4.4‰ to −1.2‰ VSMOW, within the range of values measured from the fluid inclusions in this study (Table 2).

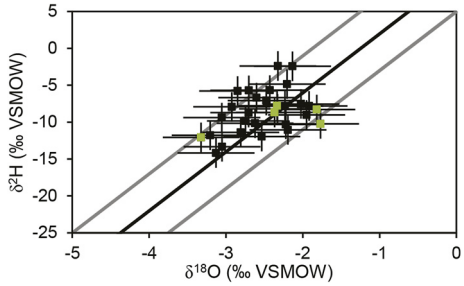

Fig. 5. The $\delta^{18}O_w$ and δ^2H_w values from fluid inclusion water isotopes plotted with the GMWL in black and ±5‰ δ^2H of the GMWL in grey. Samples shown in green represent fluid inclusion samples analyzed across Heinrich stadials. Samples all fall near the GMWL suggesting that the water isotopes have not been significantly fractionated due to evaporation. (For interpretation of the references to color in this figure legend, the reader is referred to the web version of this article.)

Table 2
Fluid inclusion oxygen and hydrogen isotope values with an average error of 0.5 and 2.0‰ respectively. Temperature was calculated from Tremaine et al. (2011), the average error of 2.7 °C was calculated by accounting for the errors on the fluid inclusion analyses.

cm from top	Age (yr BP)	Average $\delta^{18}O_w$ ‰ (VSMOW) ±0.5‰	Average δ^2H_w ‰ (VSMOW) ±2.0‰	*n*	$\delta^{18}O_c$ ‰ (VPDB)	Temperature[a] (°C) ±2.7 °C
0.9	14 125	−2.7	−9.8	2	−2.3	17.3
3.0	14 770	−2.3	−2.4	2	−1.6	15.8
3.6	14 877	−2.2	−4.8	2	−1.6	16.1
4.8	15 459	−2.4	−8.7	3	−1.0	12.2
5.5	16 648	−2.3	−7.8	1	−0.7	11.3
6.0	17 125	−2.2	−11.1	3	−2.2	19.7
6.6	17 290	−2.5	−12.0	1	−2.1	17.5
7.2	17 384	−2.8	−5.8	2	−2.0	15.3
8.0	17 458	−3.1	−13.3	2	−2.0	13.9
8.5	17 517	−2.5	−7.1	2	−2.2	18.1
10.1	18 223	−2.7	−5.7	2	−2.4	17.7
10.6	18 634	−2.8	−11.4	2	−2.3	16.8
11.1	19 111	−2.4	−5.7	3	−2.3	18.6
11.6	19 416	−3.1	−9.4	2	−2.1	14.8
12.7	20 060	−3.2	−11.8	1	−2.5	15.9
13.6	21 470	−2.6	−10.2	2	−2.5	18.8
14.5	22 044	−2.4	−8.7	2	−1.9	17.0
14.9	23 191	−3.1	−14.2	1	−2.1	14.4
15.4	25 259	−3.3	−12.1	1	−2.0	12.8
16.0	26 011	−2.9	−7.9	3	−1.6	12.6
17.7	26 369	−2.7	−8.7	2	−2.1	16.6
18.3	26 550	−2.3	−8.2	1	−2.0	17.9
19.1	26 846	−2.0	−7.5	2	−2.4	21.7
19.4	26 972	−2.6	−6.7	2	−2.5	18.7
19.9	27 176	−1.9	−9.0	2	−2.2	20.7
20.5	27 483	−1.9	−7.8	2	−2.5	22.4
21.0	27 877	−2.2	−10.3	3	−2.2	19.5
21.5	28 549	−2.2	−7.8	2	−2.0	18.1
22.0	29 639	−2.1	−2.4	2	−2.2	19.8
22.4	30 672	−1.8	−10.2	2	−2.1	21.5
22.8	31 733	−1.8	−8.3	2	−1.4	17.4

[a] Temperature calculated from Tremaine et al. (2011).

3.3. Carbon and oxygen isotopes of carbonate

The speleothem AB-DC-09 was sampled at both high (one sample every ∼2 yr) and low resolution (one sample every ∼50 yr). To aid with the analysis of the data, the $\delta^{13}C$ and $\delta^{18}O$ carbonate isotope results are plotted with a 50-year interpolation (Fig. 4a and b). A comparison of the $\delta^{13}C$ and $\delta^{18}O$ of the speleothem calcite ($\delta^{18}O_c$ and $\delta^{13}C_c$) with the derived age model demonstrates significant variations in the isotopic value of the calcite (Fig. 4a and b). The variation in the $\delta^{13}C_c$ results are 6.2‰ for the sample, with the most positive $\delta^{13}C_c$ value of +3.2‰ VPDB occurring at 31.7 ± 1 kyr BP. Above average $\delta^{13}C_c$ values are also found at 15 ± 0.2 kyr and 25 ± 0.2 kyr BP (Fig. 4a). Similar results are

found in the $\delta^{18}O_c$ record with the most positive $\delta^{18}O_c$ value of −0.2‰ VPDB at 15 ± 0.2 kyr and above average $\delta^{18}O_c$ values at 24.1 ± 0.2 kyr and 31.5 ± 1 kyr BP (Fig. 4b). Overall, a total of 3.5‰ variation is observed in the $\delta^{18}O_c$ results. A similar trend for each positive C and O isotope event is observed, with a gradual increase leading to a maximum, followed by a more rapid decline. For the 15 kyr event, the gradual increase begins at 17.4 kyr BP and reaches a maximum at ∼15 kyr BP, followed by a rapid decrease (∼200 yr) in $\delta^{18}O_c$ and $\delta^{13}C_c$ values. The trend is also observed across the 24.5 kyr event with an increase beginning at ∼26 kyr BP to a maximum, followed by a decrease. For the oldest event, maximum $\delta^{18}O_c$ and $\delta^{13}C_c$ values occurred at ∼31.5 kyr and declined over ∼200 yr after the maximum. In summary, the carbonate results support three unique shifts, of which the least significant in both $\delta^{13}C_c$ and $\delta^{18}O_c$ is the 24.5 kyr BP event (Fig. 4a and b).

3.4. Fluid inclusions

A comparison of the $\delta^{18}O_w$ measured on the fluid inclusions with the derived age model from U–Th geochronometry demonstrates minimal variations in the isotopic value of the fluids (Fig. 4c). The $\delta^{2}H_w$ and $\delta^{18}O_w$ measured on the fluid inclusions support variations of 11.7‰ and 1.6‰ respectively, over the studied interval with average values of −8.6‰ $\delta^{2}H_w$ and −2.5‰ $\delta^{18}O_w$ VSMOW (Table 2). The variability in the $\delta^{18}O_w$ value is relatively small compared to the changes in the $\delta^{18}O_c$ value (∼3.5‰, Fig. 4c). The data support a minimum $\delta^{18}O_w$ value at 25.3 kyr BP and a maximum $\delta^{18}O_w$ value at 30.7 kyr BP. Fluid inclusion samples formed during Heinrich stadial 1 include two samples at 15.5 and 16.6 kyr BP, Heinrich stadial 2 includes one sample at 25.3 kyr BP and Heinrich stadial three includes one sample at 31.7 kyr BP (Fig. 3).

4. Discussion

4.1. Climate interpretation of the oxygen isotope record: aridity vs. temperature

The $\delta^{18}O_w$ values of the fluid inclusions shows an overall 1.6‰ decline from 30.7 to 25.3 kyr BP. Decreases in $\delta^{18}O_w$ are generally attributed to the 'amount' effect (Dansgaard, 1964) and therefore this change suggests an increase in the amount of precipitation over this period, an interpretation supported by a progressively increasing growth rate. The $\delta^{18}O_c$ record shows a maxima at $\sim 15 \pm 0.2$, 24.1 ± 0.2, and 31.5 ± 1 kyr BP and the timing of these events is associated with Heinrich stadials 1, 2, and 3 (Fig. 6). In contrast to a significant increase of $\delta^{18}O_c$ values within each of the three Heinrich stadials, the $\delta^{18}O_w$ data obtained from the fluid inclusions reveals only minimal changes. For example, the average change in the $\delta^{18}O_w$ value across Heinrich stadial 1, from 17.1 to 14.8 kyr BP, is 0.2‰ which is less than the analytical uncertainty. The average change from 26 to 23 kyr BP is 0.4‰ for $\delta^{18}O_w$ value (Fig. 4c). The minimal change in the $\delta^{18}O_w$ data (Fig. 4c, g) suggests that the amount of rainfall did not significantly change during Heinrich stadials. The increase in $\delta^{18}O_c$ values across the Heinrich stadials, which is much greater than that found in the $\delta^{18}O_w$ results, most likely arises from lower temperatures, rather than a significant change in the $\delta^{18}O_w$ value or precipitation amount. The $\delta^{18}O_w$ values, when combined with $\delta^{18}O_c$ values, allows for the calculation of the temperature at the time of mineral formation. Through the application of the cave-specific water–calcite oxygen isotope fractionation relationship from Tremaine et al. (2011), temperature has been calculated using the measured $\delta^{18}O_w$ and $\delta^{18}O_c$ values. The equation is as follows:

$$1000 \ln \alpha = 16.1\left(10^3 T^{-1}\right) - 24.6 \quad (1)$$

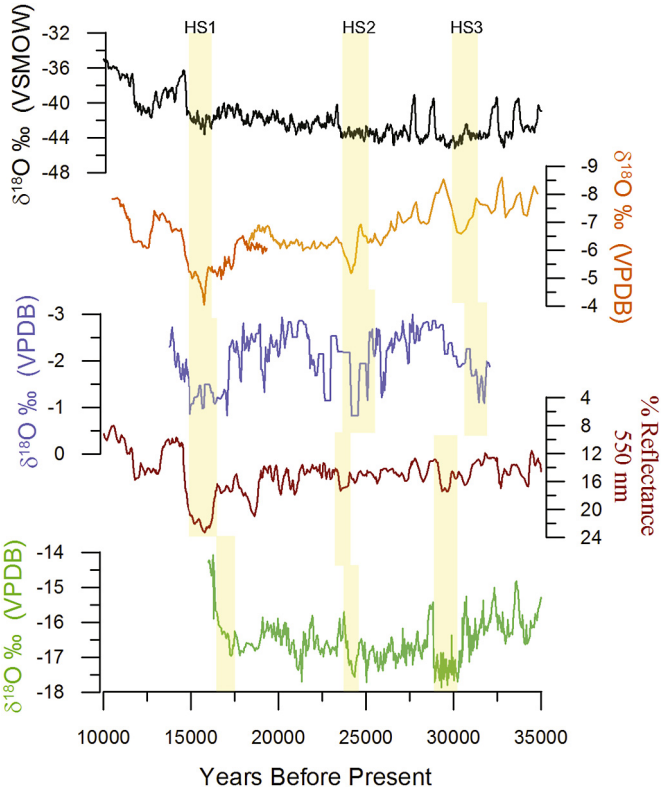

Fig. 6. Compilation of paleoclimate studies from throughout the Atlantic. a) $\delta^{18}O$ time series from NGRIP ice core (black) data from Wolff et al. (2010) plotted with a 5 point running average. b) In orange, $\delta^{18}O$ time series from Hulu Cave, China data from PD and MSD samples from Wang et al. (2001) note the axis is reversed. c) Oxygen isotope time series from this study (sample AB-DC-09) plotted with a 50 yr interpolation. Note the axis is reversed. d) Cariaco Basin reflectance (red) at 550 nm, axis reversed from Peterson et al. (2000) with a 5 point smoothing. e) Green is $\delta^{18}O$ record from Pacupahuain Cave, Peru from Kanner et al. (2012). (For interpretation of the references to color in this figure legend, the reader is referred to the web version of this article.)

With α representing the fractionation factor between two substances (in this case the measured water and calcite oxygen isotopes) and T in Kelvin (Tremaine et al., 2011). Equation (1) was developed from a cave monitoring study in Florida, and was found to be in good agreement with caves throughout the world (Tremaine et al., 2011).

While caves generally maintain a constant temperature throughout the year (representative of mean annual temperature), over longer time periods, speleothems can record decadal to centennial scale changes in temperature. Utilizing equation (1), the average temperature (not including the samples forming over Heinrich stadials, as defined in Section 3.4) was 17.7 ± 2.7 °C. This average temperature is cooler than the average modern annual temperature for the Bahamas (average annual temperature = 22 to 28 °C, Baldini et al., 2007) and typical temperatures within modern dry caves in the area (average annual cave temperature = 23.2 °C, Arienzo et al., 2013). Heinrich stadials 1, 2, and 3 are represented by cooler temperatures, with the average temperature across Heinrich stadials 1, 2 and 3 of 13.4 ± 2.7 °C, representing an average temperature decrease of 4.3 ± 2.7 °C and Heinrich stadial 1 being the coolest event (Fig. 4d).

4.2. Climate interpretation of the carbon isotope record

Both the $\delta^{13}C_c$ and $\delta^{18}O_c$ results consists of increased values around 15 ± 0.2, 24.5 ± 0.2, and 31.6 ± 1 kyr BP suggesting that similar environmental factors influenced the $\delta^{13}C_c$ and $\delta^{18}O_c$ composition of the stalagmite during Heinrich stadials. As the $\delta^{18}O_c$

value across Heinrich stadial events is primarily driven by changes in the cave temperature, we suggest that the increases in the $\delta^{13}C_c$ values are indirectly driven by cooling during these Heinrich stadials. Assuming changes in cave ventilation did not occur during sample deposition, the $\delta^{13}C_c$ ratio of the speleothem is most likely driven by changes in the soil zone or the vegetation above the cave. The increased $\delta^{13}C_c$ values may be a result of a decline in soil microbial activity, which tends to increase the $\delta^{13}C_{DIC}$ ratio (Dissolved Inorganic Carbon, DIC) of the drip water during periods of cooler temperatures. Support for this notion comes from similar results found in a cave in France, where lower $\delta^{13}C_c$ values during warm periods were driven by drip water having a greater biogenic CO_2 component (Genty et al., 2003). Nevertheless, it is not possible to rule out the potential influence of changes in the amount of precipitation on the $\delta^{13}C_c$ record. An increase in the $\delta^{13}C_c$ ratio of the carbonate can be driven by aridity, which leads to a reduction in soil microbial activity, or a greater proportion of C_4 versus C_3 plants. While this is a valid interpretation of the carbon isotope results, the oxygen isotope results from fluid inclusion analysis do not suggest a reduction in the amount of rainfall as a driver of the $\delta^{18}O_c$ record.

4.3. Climate variability in the context of the Atlantic Basin

Proxy records from throughout the Atlantic not only support significant climate shifts associated with Heinrich stadials, but they are also in good agreement with the timing of Heinrich stadials 1–3 (Fig. 6). These reconstructions support the global scale response to Heinrich stadials. The difference in climate expression between Northern Hemisphere records (e.g., Hulu Cave, Cariaco Basin, and the Bahamas) compared to Southern Hemisphere records (e.g., Pacupahuain Cave) demonstrates the anti-phased response across Heinrich stadials (Broecker, 1998; Kanner et al., 2012; Peterson et al., 2000; Wang et al., 2001, 2004) (Fig. 6). This anti-phased relationship between the hemispheres is in part due to a shift in climate across Heinrich stadials and is well documented in the ice core records with the Greenland ice core records supporting cooling and the ice cores from Antarctica supporting warming during Heinrich stadials (Broecker, 1998; Wolff et al., 2010).

The Bahamian speleothem record, along with other proxies from the subtropical/tropical western Atlantic, support overall drying and/or similar cooling associated with Heinrich stadials (Escobar et al., 2012; Lachniet et al., 2013; Peterson et al., 2000) (Fig. 6). This coherence in climate expression among the North Atlantic tropical records across Heinrich stadials can be explained by a regional shift in climate. An alkenone-derived SST record from the Bermuda Rise across Heinrich stadials 4 and 5 shows a $\sim$ 3–5 °C decrease in SSTs (Sachs and Lehman, 1999) suggesting SSTs also may have declined during earlier Heinrich stadials. Further south, a lake record from Guatemala shows an increased aridity and a 6–10 °C cooling associated with Heinrich stadial 1 (Escobar et al., 2012; Hodell et al., 2012). The temperatures observed during Heinrich stadial 1 are lower than the modern mean annual temperature for Guatemala (mean annual temperature = 26 °C) (Hodell et al., 2012) and the increased aridity and cooling in Guatemala is thought to be driven by a southerly shifted ITCZ and decreased tropical Atlantic SSTs (Escobar et al., 2012; Hodell et al., 2012). The amount of cooling observed in the Guatemala and the Bermuda records (between 3–10 °C) across Heinrich stadials is similar to the amount of cooling observed in the Bahamas record presented here ($\sim$4 °C). Modeling results also support decreased temperatures for the tropical Northern Hemisphere coincident with Heinrich stadials, however, the modeled temperature changes are much less (Murphy et al., 2014; Zhang and Delworth, 2005).

As suggested above, while the geochemical data in the speleothem record from the Bahamas supports a decrease in temperature, the carbon isotope results do not rule out the possibility of enhanced aridity across these events, which potentially may drive the variability in the carbon isotopic record. A speleothem record from southwestern Mexico demonstrates a reduction in the North American Monsoon associated with Heinrich stadial 1 driven by the southerly shifted ITCZ and reduced AMOC (Lachniet et al., 2013). A southerly shift in the ITCZ would be accompanied by an expanded Bermuda high, which could have led to increased aridity in the Bahamas across Heinrich stadials (Hodell et al., 2000).

In contrast to the data presented here, a record based on pollen from Lake Tulane, Florida in the southeastern U.S. suggests warmer and wetter Heinrich stadials (Grimm et al., 2006). These authors attributed the warming and increased rainfall to a slowdown of the AMOC leading to a reduction in the transport of heat from the Gulf of Mexico and thereby forcing the observed warmer and wetter climate in Florida (Grimm et al., 2006). This climate response may not be observed in the Bahamas as a result of the location of Abaco Island, on the eastern edge of the Bahamas platform, and therefore this study site may not have been influenced by changes in the Gulf of Mexico. Furthermore, the postulated warming of the Gulf of Mexico from the Florida record is not consistent with the simulated climate response to an AMOC shut down rather, most climate models suggest a cooling of the entire North Atlantic, including the Gulf of Mexico (Clement and Peterson, 2008, and references therein).

In many paleoclimate proxy reconstructions, Heinrich stadial 1 is a larger magnitude event compared to stadials 2 and 3 (Stager et al., 2011). In the record presented here, Heinrich stadial 1 is characterized by the greatest change in $\delta^{18}O_c$ and temperature (observed $\sim$5.9 °C temperature decrease) (Fig. 6). Heinrich stadial 2 exhibits minimal geochemical changes which may be due to a minimal change in the AMOC during this event (Lynch-Stieglitz et al., 2014; McManus et al., 2004). While Heinrich stadial 1 has been shown to be the strongest event in many paleoclimate reconstructions, it is also a period punctuated with climate changes. For example, in Guatemala a lake record indicates a cold and dry period beginning around 18 kyr BP, interrupted by a wetter and warmer period $\sim$17 kyr BP, and followed by a return to drier and cooler temperatures at approximately 16.1 kyr BP (Escobar et al., 2012; Hodell et al., 2012). The authors suggest the two cold and dry periods observed in Guatemala are driven by two separate North Atlantic IRD events (Escobar et al., 2012). Similar to the observations in Guatemala, a multi-proxy study of a core from the Cariaco Basin supports the drier climate associated with Heinrich stadial 1 is interrupted by a shift to wetter climate conditions (Escobar et al., 2012; Yurco, 2010). In this speleothem record from the Bahamas, geochemical results suggest a temperature increase and/or precipitation change from $\sim$17.5 to $\sim$17.1 kyr BP followed by a progressively cooler Heinrich stadial 1 period (Table 2, Fig. 4g and h). These results suggest that Heinrich stadial 1 in the tropical North Atlantic may exhibit centennial scale climate oscillations associated with high latitude IRD events.

Additional $\delta^{18}O_c$ and $\delta^{13}C_c$ variations, not associated with Heinrich stadials, are observed at 19.1 ± 0.2 and 22.6 ± 0.2 kyr before present. The magnitude of the isotopic shifts at 19 and 22.6 kyr BP are less than the isotopic shifts observed during Heinrich stadial events (at 19 kyr BP, a 1.7‰ shift in the $\delta^{13}C_c$ value and at 22.6 kyr BP a 2‰ shift for $\delta^{13}C_c$). Both of these time periods are also associated with a minor increase in temperature and $\delta^{18}O_w$ value from the fluid inclusion results. Similarly, Bond et al. (1997) observed increased IRD deposits at similar time periods potentially suggesting these isotopic variations are associated with high latitude events.

The resumption of AMOC at the end of Heinrich stadial 1 is believed to have resulted in an increase in SSTs in the North Atlantic (McManus et al., 2004), leading to the northward shift of the ITCZ and the observed shift to wetter and warmer conditions in the northern tropics and the start of the Bølling–Allerød period (Peterson et al., 2000). This is also supported by the increase in temperatures after Heinrich stadial 1 from the fluid inclusion results (Fig. 4d).

While other climate records for the same time period from nearby localities such as the Cariaco Basin (Peterson et al., 2000) and stalagmites from the Peruvian Andes (Kanner et al., 2012) have recorded millennial scale variations (e.g., D/O events) there is no evidence of D/O variability in the isotopic record of sample AB-DC-09. A similar observation was made from speleothems collected from Borneo in which the geochemistry of the speleothems recorded Heinrich stadials, but not the D/O events (Carolin et al., 2013). The lack of evidence for D/O events suggests that these are different to Heinrich stadials either in the forcing mechanism, the global propagation, the geographic expression, or how these events are recorded in the speleothems, and also supports the significant impact of Heinrich stadials on tropical climate (Carolin et al., 2013; Wang et al., 2004).

5. Conclusion

The stalagmite record reported in this paper reveals three distinctive climate changes during the last glacial period, each coincident with a Heinrich stadial. The $\delta^{18}O_c$ and $\delta^{13}C_c$ data support significant shifts within the Heinrich stadials, while minimal changes occur in the $\delta^{18}O$ of the water contained in fluid inclusions. The $\delta^{18}O$ of the carbonate and the fluid inclusion results demonstrate that Heinrich stadials 1–3 are characterized by a temperature decrease, rather than an increase in aridity at this time. The observed temperature decreases are consistent with paleoclimate records from the Western Atlantic and we propose that the average temperature decline of $\sim$4 °C during Heinrich stadials is due to the meridional shift in the Northern Hemisphere climate that led to cooler subtropics. Finally, the results support the teleconnection between the subtropical Atlantic and cooling in the North Atlantic and the sensitivity of the Bahamas to changes in AMOC.

Acknowledgements

This research was supported with funds from NSF grant AGS-1103489 (PKS, AC, KB, and AP), a Geological Society of America Graduate Student Research Grant # 9575-11 to MMA and a grant from The National Geographic Society # EC0428-09 to KB and BK. The authors would like to thank the Stable Isotope Laboratory members at the University of Miami for insightful discussions and assistance with sample analysis and G. MacKenzie for her editorial advice. The authors would also like to thank the reviewers for their comments, which greatly enhanced the paper.

Appendix A. Supplementary material

Supplementary material related to this article can be found online at http://dx.doi.org/10.1016/j.epsl.2015.08.035.

References

Arienzo, M.M., Swart, P.K., Vonhof, H.B., 2013. Measurement of $\delta^{18}O$ and $\delta^{2}H$ values of fluid inclusion water in speleothems using cavity ring-down spectroscopy compared with isotope ratio mass spectrometry. Rapid Commun. Mass Spectrom. 27, 2616–2624.

Asmerom, Y., Polyak, V.J., Burns, S.J., 2010. Variable winter moisture in the southwestern United States linked to rapid glacial climate shifts. Nat. Geosci. 3, 114–117.

Baldini, L.M., Walker, S.E., Railsback, L.B., Baldini, J.U.L., Crowe, D.E., 2007. Isotopic ecology of the modern land snail Cerion, San Salvador, Bahamas: preliminary advances toward establishing a low-latitude island paleoenvironmental proxy. Palaios 22, 174–187.

Beck, J.W., Richards, D.A., Edwards, R.L., Silverman, B.W., Smart, P.L., Donahue, D.J., Hererra-Osterheld, S., Burr, G.S., Calsoyas, L., Jull, A.J., Biddulph, D., 2001. Extremely large variations of atmospheric ^{14}C concentration during the last glacial period. Science 292, 2453–2458.

Bond, G., Showers, W., Cheseby, M., Lotti, R., Almasi, P., deMenocal, P., Priore, P., Cullen, H., Hajdas, I., Bonani, G., 1997. A pervasive millennial-scale cycle in North Atlantic Holocene and glacial climates. Science 278, 1257–1266.

Breitenbach, S., Rehfeld, K., Goswami, B., Baldini, J., Ridley, H., Kennett, D., Prufer, K., Aquino, V., Asmerom, Y., Polyak, V., Cheng, H., Kurths, J., Marwan, N., 2012. COnstructing Proxy Records from Age models (COPRA). Clim. Past 8, 1765–1779.

Broecker, W.S., 1998. Paleocean circulation during the last deglaciation: a bipolar seesaw? Paleoceanography 13, 119–121.

Carolin, S.A., Cobb, K.M., Adkins, J.F., Clark, B., Conroy, J.L., Lejau, S., Malang, J., Tuen, A.A., 2013. Varied response of western Pacific hydrology to climate forcings over the last glacial period. Science 340, 1564–1566.

Chiang, J.C.H., Bitz, C.M., 2005. Influence of high latitude ice cover on the marine Intertropical Convergence Zone. Clim. Dyn. 25, 477–496.

Clement, A.C., Peterson, L.C., 2008. Mechanisms of abrupt climate change of the last glacial period. Rev. Geophys. 46.

Craig, H., 1961. Isotopic variations in meteoric waters. Science 133, 1702–1703.

Dansgaard, W., 1964. Stable isotopes in precipitation. Tellus 16, 436–468.

Dansgaard, W., Johnsen, S.J., Clausen, H.B., Dahl-Jensen, D., Gundestrup, N., Hammer, C.U., Oeschger, H., 1984. North Atlantic climatic oscillations revealed by deep Greenland ice cores. In: Climate Processes and Climate Sensitivity. AGU, p. 10.

Dorale, J.A., Liu, Z.H., 2009. Limitations of Hendy Test criteria in judging the paleoclimatic suitability of speleothems and the need for replication. J. Caves Karst Stud. 71, 73–80.

Edwards, R.L., Gallup, C.D., Cheng, H., 2003. U-series dating of marine and lacustrine carbonates. In: Bourdon, B. (Ed.), Reviews in Mineralogy and Geochemistry: Uranium Series Geochemistry. Mineralogical Society of America, Washington, DC.

Escobar, J., Hodell, D.A., Brenner, M., Curtis, J.H., Gilli, A., Mueller, A.D., Anselmetti, F.S., Ariztegui, D., Grzesik, D.A., Perez, L., Schwalb, A., Guilderson, T.P., 2012. A $\sim$43-ka record of paleoenvironmental change in the Central American lowlands inferred from stable isotopes of lacustrine ostracods. Quat. Sci. Rev. 37, 92–104.

Fairchild, I.J., Smith, C.L., Baker, A., Fuller, L., Spötl, C., Mattey, D., McDermott, F., E.I.M.F., 2006. Modification and preservation of environmental signals in speleothems. Earth-Sci. Rev. 75, 105–153.

Fietzke, J., Liebetrau, V., Eisenhauer, A., Dullo, C., 2005. Determination of uranium isotope ratios by multi-static MIC-ICP-MS: method and implementation for precise U- and Th-series isotope measurements. J. Anal. At. Spectrom. 20, 395–401.

Genty, D., Blamart, D., Ouahdi, R., Gilmour, M., Baker, A., Jouzel, J., Van-Exter, S., 2003. Precise dating of Dansgaard–Oeschger climate oscillations in western Europe from stalagmite data. Nature 421, 833–837.

Grimm, E.C., Watts, W.A., Jacobson Jr., G.L., Hansen, B.C.S., Almquist, H.R., Dieffenbacher-Krall, A.C., 2006. Evidence for warm wet Heinrich events in Florida. Quat. Sci. Rev. 25, 2197–2211.

Hagen, S., Keigwin, L.D., 2002. Sea-surface temperature variability and deep water reorganisation in the subtropical North Atlantic during Isotope Stage 2–4. Mar. Geol. 189, 145–162.

Heinrich, H., 1988. Origin and consequences of cyclic ice rafting in the Northeast Atlantic-Ocean during the past 130,000 years. Quat. Res. 29, 142–152.

Hendy, C.H., 1971. The isotopic geochemistry of speleothems—I. The calculation of the effects of different modes of formation on the isotopic composition of speleothems and their applicability as palaeoclimatic indicators. Geochim. Cosmochim. Acta 35, 801–824.

Hodell, D.A., Brenner, M.K., Curtis, J.H., 2000. Climate change in the northern American tropics and subtropics since the last ice age: implications for environment and culture. In: Lentz, D.L. (Ed.), Imperfect Balance: Landscape Transformations in the Pre-Columbian Americas. Columbia University Press, New York, pp. 13–38.

Hodell, D.A., Turchyn, A.V., Wiseman, C.J., Escobar, J., Curtis, J.H., Brenner, M., Gilli, A., Mueller, A.D., Anselmetti, F., Ariztegui, D., Brown, E.T., 2012. Late Glacial temperature and precipitation changes in the lowland Neotropics by tandem measurement of $\delta^{18}O$ in biogenic carbonate and gypsum hydration water. Geochim. Cosmochim. Acta 77, 352–368.

Hoffmann, D.L., Beck, J.W., Richards, D.A., Smart, P.L., Singarayer, J.S., Ketchmark, T., Hawkesworth, C.J., 2010. Towards radiocarbon calibration beyond 28 ka using speleothems from the Bahamas. Earth Planet. Sci. Lett. 289, 1–10.

Kanner, L.C., Burns, S.J., Cheng, H., Edwards, R.L., 2012. High-latitude forcing of the South American summer monsoon during the Last Glacial. Science 335, 570–573.

Keigwin, L.D., Jones, G.A., 1994. Western North-Atlantic evidence for millennial-scale changes in ocean circulation and climate. J. Geophys. Res. Oceans 99, 12397–12410.

Lachniet, M.S., 2009. Climatic and environmental controls on speleothem oxygen-isotope values. Quat. Sci. Rev. 28, 412–432.

Lachniet, M.S., Asmerom, Y., Bernal, J.P., Polyak, V.J., Vazquez-Selem, L., 2013. Orbital pacing and ocean circulation-induced collapses of the Mesoamerican monsoon over the past 22,000 y. Proc. Natl. Acad. Sci. USA 110, 9255–9260.

Lynch-Stieglitz, J., Schmidt, M.W., Henry, L.G., Curry, W.B., Skinner, L.C., Mulitza, S., Zhang, R., Chang, P., 2014. Muted change in Atlantic overturning circulation over some glacial-aged Heinrich events. Nat. Geosci. 7, 144–150.

McGee, D., Quade, J., Edwards, R.L., Broecker, W.S., Cheng, H., Reiners, P.W., Evenson, N., 2012. Lacustrine cave carbonates: novel archives of paleohydrologic change in the Bonneville Basin (Utah, USA). Earth Planet. Sci. Lett. 351, 182–194.

McManus, J.F., Francois, R., Gherardi, J.M., Keigwin, L.D., Brown-Leger, S., 2004. Collapse and rapid resumption of Atlantic meridional circulation linked to deglacial climate changes. Nature 428, 834–837.

Mühlinghaus, C., Scholz, D., Mangini, A., 2009. Modelling fractionation of stable isotopes in stalagmites. Geochim. Cosmochim. Acta 73, 7275–7289.

Murphy, L.N., Clement, A.C., Albani, S., Mahowald, N.M., Swart, P.K., Arienzo, M.M., 2014. Simulated changes in atmospheric dust in response to a Heinrich stadial. Paleoceanography 29, 30–43.

Peterson, L.C., Haug, G.H., Hughen, K.A., Rohl, U., 2000. Rapid changes in the hydrologic cycle of the tropical Atlantic during the last glacial. Science 290, 1947–1951.

Pourmand, A., Tissot, F.L.H., Arienzo, M.M., Sharifi, A., 2014. Introducing a comprehensive data reduction and uncertainty propagation algorithm for U–Th geochronometry with extraction chromatography and isotope dilution MC-ICP-MS. Geostand. Geoanal. Res. 38, 129–148.

Richards, D.A., Smart, P.L., Edwards, R.L., 1994. Maximum sea levels for the last glacial period from U-series ages of submerged speleothems. Nature 367, 357–360.

Roberts, W., Valdes, P., Payne, A., 2014. Topography's crucial role in Heinrich Events. Proc. Natl. Acad. Sci. USA 111, 16688–16693.

Robinson, L.F., Belshaw, N.S., Henderson, G.M., 2004. U and Th concentrations and isotope ratios in modern carbonates and waters from the Bahamas. Geochim. Cosmochim. Acta 68, 1777–1789.

Sachs, J.P., Lehman, S.J., 1999. Subtropical North Atlantic temperatures 60,000 to 30,000 years ago. Science 286, 756–759.

Stager, J.C., Ryves, D.B., Chase, B.M., Pausata, F.S., 2011. Catastrophic drought in the Afro-Asian monsoon region during Heinrich event 1. Science 331, 1299–1302.

Tremaine, D.M., Froelich, P.N., Wang, Y., 2011. Speleothem calcite farmed in situ: modern calibration of $\delta^{18}O$ and $\delta^{13}C$ paleoclimate proxies in a continuously-monitored natural cave system. Geochim. Cosmochim. Acta 75, 4929–4950.

van Breukelen, M.R., Vonhof, H.B., Hellstrom, J.C., Wester, W.C.G., Kroon, D., 2008. Fossil dripwater in stalagmites reveals Holocene temperature and rainfall variation in Amazonia. Earth Planet. Sci. Lett. 275, 54–60.

Walker, L.N., Mylroie, J.E., Walker, A.D., Mylroie, J.R., 2008. The caves of Abaco Island, Bahamas: keys to geologic timelines. J. Caves Karst Stud. 70, 108–119.

Wang, X., Auler, A.S., Edwards, R.L., Cheng, H., Cristalli, P.S., Smart, P.L., Richards, D.A., Shen, C.C., 2004. Wet periods in northeastern Brazil over the past 210 kyr linked to distant climate anomalies. Nature 432, 740–743.

Wang, Y.J., Cheng, H., Edwards, R.L., An, Z.S., Wu, J.Y., Shen, C.C., Dorale, J.A., 2001. A high-resolution absolute-dated late Pleistocene monsoon record from Hulu Cave, China. Science 294, 2345–2348.

Wolff, E.W., Chappellaz, J., Blunier, T., Rasmussen, S.O., Svensson, A., 2010. Millennial-scale variability during the last glacial: the ice core record. Quat. Sci. Rev. 29, 2828–2838.

Yurco, L.N., 2010. A multi-proxy investigation of the late glacial "Mystery Interval" (17.5–14.5 ka) in the Cariaco Basin, Venezuela. MS Thesis. Marine Geology and Geophysics, University of Miami.

Zhang, R., Delworth, T.L., 2005. Simulated tropical response to a substantial weakening of the Atlantic thermohaline circulation. J. Climate 18, 1853–1860.